

Anomalous velocity distributions in active Brownian suspensions

Andrea Fiege,¹ Benjamin Vollmayr-Lee,² and Annette Zippelius^{1,3}

¹*Georg-August-Universität Göttingen, Institut für Theoretische Physik, Friedrich-Hund-Platz 1, 37077 Göttingen, Germany*

²*Department of Physics and Astronomy, Bucknell University, Lewisburg, Pennsylvania 17837, USA*

³*Max-Planck-Institut für Dynamik und Selbstorganisation, Am Fassberg 17, 37077 Göttingen, Germany*

(Received 4 March 2013; published 21 August 2013)

Large-scale simulations and analytical theory have been combined to obtain the nonequilibrium velocity distribution, $f(v)$, of randomly accelerated particles in suspension. The simulations are based on an event-driven algorithm, generalized to include friction. They reveal strongly anomalous but largely universal distributions, which are independent of volume fraction and collision processes, which suggests a one-particle model should capture all the essential features. We have formulated this one-particle model and solved it analytically in the limit of strong damping, where we find that $f(v)$ decays as $1/v$ for multiple decades, eventually crossing over to a Gaussian decay for the largest velocities. Many particle simulations and numerical solution of the one-particle model agree for all values of the damping.

DOI: [10.1103/PhysRevE.88.022138](https://doi.org/10.1103/PhysRevE.88.022138)

PACS number(s): 05.20.Jj, 47.57.J–, 47.63.Gd, 47.70.Nd

I. INTRODUCTION

In recent years there has been growing interest in so called active matter, referring to the ability of the constituents to move actively by either extracting energy from the environment or depleting an internal energy depot. Examples are motor proteins, bacterial swimmers, or motile cells [1]. Whereas the mechanism that drives the individual active particle has been studied for many years [2–4], the collective behavior of a large number of individuals has been addressed only recently. Very rich behavior has been observed, ranging from pattern formation and nonequilibrium phase transitions to turbulence [5,6]. Active particles on mesoscopic to macroscopic scales have also been realized in the form of self-propelled colloids (Janus particles) [7] and vibrated polar granular rods [8]. More generally, granular particles that are driven by random kicks may be considered active matter with, however, the direction of motion being random.

Our focus here are the velocity distributions of active particles in suspension. Whereas in equilibrium, the velocities universally follow the Maxwell-Boltzmann distribution, this does not hold for nonequilibrium stationary states, where in general deviations from the Maxwell-Boltzmann distribution are observed. Few studies have focused on the velocity distribution in the context of active cell and bacteria suspensions [9,10]. In Ref. [9] extensive experimental data were taken for several cell types, allowing for a statistical analysis of the cell's velocities. The authors concluded that exponential distributions are a general characteristic feature of cell motility. Such exponential distributions have indeed been found in models of active Brownian particles [11]; however other distributions have been seen as well, depending on the mechanism of self-propulsion [11,12].

For driven granular media on the other side, numerous studies have been performed to analyze velocity distributions. In experiments, various driving mechanisms were shown to produce non-Gaussian velocity distributions [13–18]. If the particle's motion is strongly damped either due to the surrounding fluid or due to collisions with the wall, the velocity distributions are exponential. In Ref. [16] the authors use a single-particle simulation of a frictional particle to explain the

observed velocity distribution. Their argument was turned into a Fokker-Planck equation [19,20], whose stationary solution is in good agreement with experiment [19].

In the present work we study a simple model of active particles in a suspension, described below, using event-driven simulations. We obtain nearly universal velocity distributions, which depend primarily on a single parameter, and which exhibit significant deviations from Gaussian behavior, but also nonexponential tails (see Fig. 1). Further, we develop a single-particle theory that shows good agreement with the simulation data.

II. MODEL

Here we discuss a simple model for active particles: hard spheres placed in a fluid with a viscous drag γ , which are accelerated at discrete times and undergo elastic collisions.

The equation of motion for particle i reads

$$\partial_t \mathbf{v}_i = -\gamma \mathbf{v}_i + \left. \frac{\Delta \mathbf{v}_i}{\Delta t} \right|_{\text{coll}} + \left. \frac{\Delta \mathbf{v}_i}{\Delta t} \right|_{D_r}. \quad (1)$$

The driving force is modeled as discrete kicks with amplitude $\Delta \mathbf{p} = m \Delta \mathbf{v}$ and frequency f_{D_r} . The components of the kick velocity, e.g., Δv_x , are drawn from a Gaussian distribution with mean 0 and variance σ^2

$$P(\Delta v_x) = \frac{1}{\sqrt{2\pi}\sigma} \exp\left(-\frac{(\Delta v_x)^2}{2\sigma^2}\right) \quad (2)$$

and for the other components accordingly. We ignore hydrodynamic interactions.

The above dynamics is a very crude approximation to the run-and-tumble behavior of bacteria, such as *E. coli* and others [21–23]. In a time interval Δt , a particle is accelerated once and subsequently performs a random motion determined by the surrounding fluid and interactions with the other particles. If the bacteria acceleration events (strokes) are sufficiently rare, subsequent kicks may be regarded as uncorrelated in direction, so that our model should apply.

We are interested in a steady state, where the energy due to dissipation is balanced by the energy input due to random

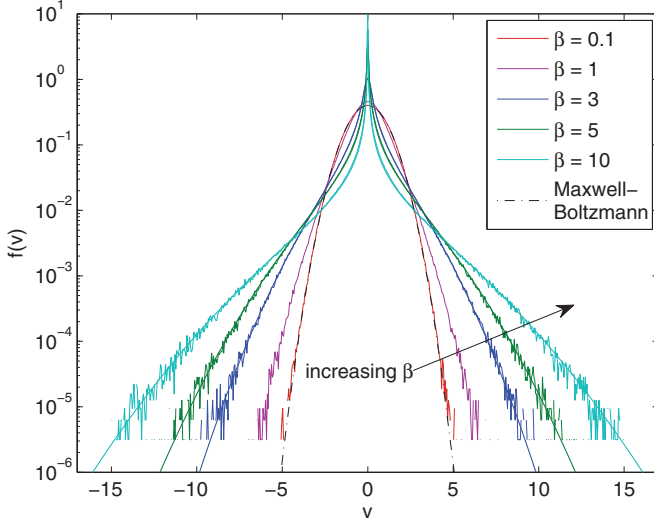


FIG. 1. (Color online) Velocity distributions for volume fraction $\eta = 0.35$, $f_{Dr} = \omega_{\text{coll}} = 7.11$, and several values of $\beta = \gamma/f_{Dr} = 0.1, 1, 3, 5, 10$. The dashed-dotted line shows the Maxwell-Boltzmann distribution. The colored solid lines show the first iterative solutions of the one-particle model (see text below) for $\beta = 3, 5, 10$.

kicks

$$2m\gamma\langle v^2 \rangle = d f_{Dr} m \sigma^2, \quad (3)$$

where d is the dimensionality of the system. In the following we will choose units such that lengths are measured in units of particle radius and mass in units of particle mass. We choose the time scale so that the average steady-state kinetic energy is $d/2$, which corresponds to $k_B T = 1$ for a thermal system. In these units the driving amplitude becomes $\sigma^2 = 2\gamma/f_{Dr}$, leaving three independent parameters: γ , f_{Dr} , and the volume fraction η . We will consider moderately dilute systems for which the particle collision frequency is well described by the Enskog result $\omega_{\text{coll}}(\eta) = 12\chi\eta/\sqrt{\pi}$ with the Carnahan-Starling expression for the pair correlation at contact $\chi = (1 - \eta/2)/(1 - \eta)^3$. Thus our three parameters provide three independent time scales: γ , f_{Dr} , and ω_{coll} (in place of η).

III. SIMULATIONS

We performed event-driven simulations of hard spheres. The original algorithm [24,25] was changed in order to implement friction as in Ref. [26]. The main effort of an event-driven simulation of ballistically moving particles goes into the calculation whether two particles will collide or not. If a collision between particle i and j will occur, the difference of their trajectories,

$$\mathbf{r}_i(t) - \mathbf{r}_j(t) \equiv \mathbf{r}_{i,j}(t) = \mathbf{r}_{i,j}(t_0) + \mathbf{v}_{i,j}(t_0)(t - t_0) \quad (4)$$

must be equal to the sum of their radii at time t_{coll} , i.e.,

$$R_i + R_j = |\mathbf{r}_{i,j}(t_{\text{coll}})| \quad (5)$$

yielding a quadratic equation in $t_{\text{coll}} - t_0$. For the damped motion, $\gamma \neq 0$, one can still integrate the equations of motion in between collisions analytically

$$\mathbf{r}_{i,j}(t) = \mathbf{r}_{i,j}(t_0) + \mathbf{v}_{i,j}(t_0) \frac{1 - e^{-\gamma(t-t_0)}}{\gamma}. \quad (6)$$

Compared to ballistic motion, the linear time interval between two collisions ($t_{\text{coll}} - t_0$) is simply replaced by $(1 - e^{-\gamma(t_{\text{coll}} - t_0)})/\gamma$. Since we know the collision time from the ballistic simulation, we can just use the above relation to determine the collision times for the damped system. The remaining events in the simulation—driving events, wall collisions, sub-box wall collisions—are handled accordingly. The only remaining difference in the damped system is that the place of a collision with another particle or a (sub-box) wall might not be within range of the damped motion. If this is the case, the collision will not occur, instead the particle will slow down until a driving event takes place.

We have simulated a three-dimensional system of 2 122 416 monodisperse spheres with volume fractions $\eta = 0.05$ and 0.35 , corresponding to $\omega_{\text{coll}} = 0.385$ and $\omega_{\text{coll}} = 7.11$. The system is equilibrated with $\gamma = 0$ and no forcing. Subsequently, damping and the acceleration force are switched on. Then, after another 100 collisions per particle to ensure relaxation to a stationary state, the velocity distribution is measured. These simulations were conducted for various values of the parameters γ , f_{Dr} , and η .

For most simulations we set the driving frequency equal to the Enskog collision frequency, $f_{Dr} = \omega_{\text{coll}}$, except for Fig. 3 where we explicitly study the effects of changing the driving frequency. The observed collision frequencies match the Enskog expression for small damping and decrease for larger damping by at most 40% for the largest damping considered here. Hence our choice, $f_{Dr} = \omega_{\text{coll}}$, implies that typically a particle collides once before it is kicked again.

In Fig. 1 we show the velocity distribution for $\eta = 0.35$ and $f_{Dr} = \omega_{\text{coll}}$ with various values of the damping constant γ . The curves are labeled by the ratio $\beta := \gamma/f_{Dr}$. Whereas for very small β the distribution is approximately Gaussian, we observe increasingly strong deviations for larger β . Small velocities are highly overpopulated with an indication of a singularity in the limit of large β . High velocities are

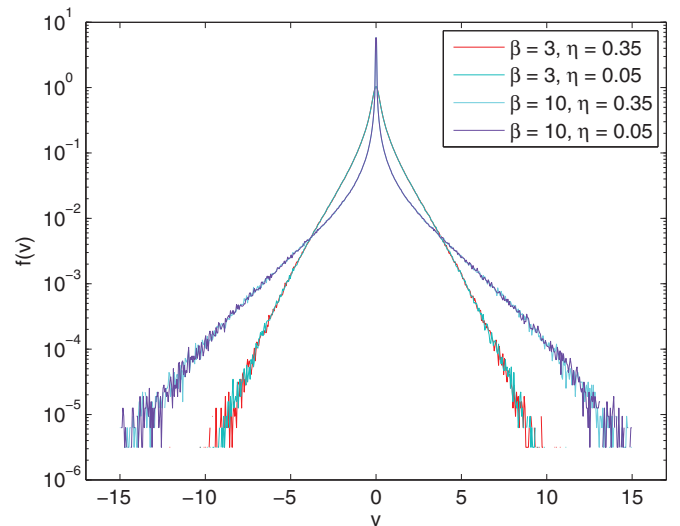


FIG. 2. (Color online) Testing the dependence of the velocity distribution on the volume fraction η . Data for $\eta = 0.05$ and $\eta = 0.35$ are shown for $\beta = 3$ and for $\beta = 10$. In both cases we find little to no dependence on the volume fraction. The driving frequency is taken to be $f_{Dr} = \omega_{\text{coll}}$.

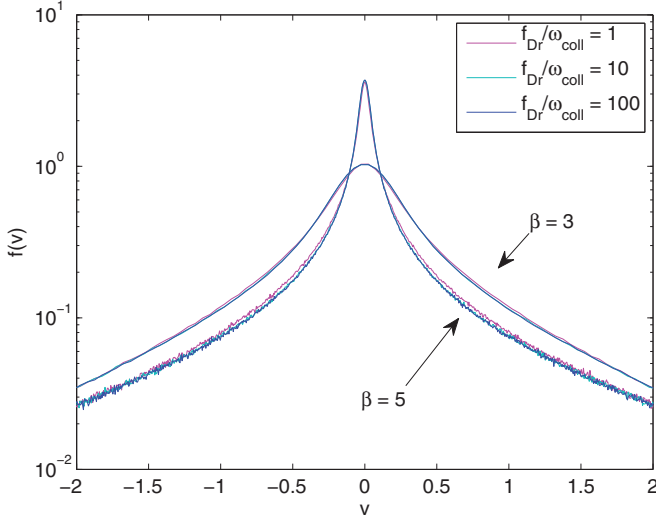


FIG. 3. (Color online) Testing the dependence of the velocity distribution on the ratio f_{Dr}/ω_{coll} for two values of β . The volume fraction is taken to be $\eta = 0.35$ corresponding to $\omega_{coll} = 7.11$.

overpopulated as well as compared to the equilibrium Maxwell-Boltzmann distribution. These deviations can be understood intuitively as follows: particles which have not been recently kicked are damped to nearly zero velocity, whereas the recently kicked particles populate the tail.

Next, we demonstrate the universality of these distributions. The three-dimensional parameter space can be spanned by the parameters η , β , and f_{Dr} . In Fig. 2 we test the volume fraction dependence of the velocity distribution. We set $f_{Dr}/\omega_{coll} = 1$ and compare for a given value of β , e.g., $\beta = 3$, the velocity distributions for two volume fractions, $\eta = 0.05$ and $\eta = 0.35$, and find no discernible difference between the distributions. This holds for all investigated values of β , and is shown in Fig. 2 for $\beta = 3$ and 10.

Then, in Fig. 3 we test the dependence of the velocity distribution on the ratio f_{Dr}/ω_{coll} . Data for $f_{Dr}/\omega_{coll} = 1, 10$, and 100 are shown for $\beta = 3$ and for $\beta = 5$. For a specific value of β , the curves for different f_{Dr}/ω_{coll} lie essentially on top of each other.

We summarize the main results of our simulations.

- (i) The distribution is independent of volume fraction for the investigated range of η .
- (ii) It is also independent of the ratio f_{Dr}/ω_{coll} ; we obtain the same distribution, no matter whether a particle is kicked once or a 100 times in between collisions.
- (iii) Consequently the distribution is almost exclusively determined by the ratio $\beta = \gamma/f_{Dr}$, even though the model contains three independent time scales, γ , f_{Dr} , and ω_{coll} .
- (iv) The one-particle velocity distribution is Gaussian only in the limit $\beta \rightarrow 0$. The distribution shows increasingly stronger deviations at small and large velocities for increasing β .
- (v) The distribution seems to develop a singularity at small argument as $\beta \rightarrow \infty$.

These observations, in particular the insensitivity to collision rate, have led us to derive an approximate analytical theory for the velocity distribution based on a single-particle model that neglects collisions.

IV. SINGLE-PARTICLE MODEL

For simplicity, we consider one spatial dimension only, assuming that the Cartesian components of the velocity are independent. With $\Delta t = 1/f_{Dr}$, we consider the time interval $[0, \Delta t)$, within which each particle gets one velocity kick at some random time. The idea of the calculation is the following: we use the one-particle distribution at the beginning of the interval as input and compute the resulting one-particle distribution at end of the interval, and then require the two distributions to be the same in the stationary state. The speed of a single particle decreases in Δt due to damping and generally increases due to a velocity kick, denoted by Δv . The kick occurs at time τ with probability $w(\tau) = \frac{1}{\Delta t}$ provided $0 \leq \tau \leq \Delta t$. We are interested in the velocity distribution at the end of the time interval, when the kick velocity has decayed to $\Delta v_f = \Delta v \exp[-\gamma(\Delta t - \tau)]$. For a given (fixed) kick size Δv , this quantity is a random variable due to the stochastic occurrence of the kick in the given time interval. The conditional probability to find a velocity Δv_f for a given kick size Δv is easily computed from the distribution $w(\tau)$

$$p_k(\Delta v_f | \Delta v) = \begin{cases} \frac{1}{\beta} \frac{1}{|\Delta v_f|}, & e^{-\beta} \leq \Delta v_f / \Delta v \leq 1 \\ 0 & \text{else.} \end{cases} \quad (7)$$

To obtain the nonconditional probability, $p_k(\Delta v_f)$ we write

$$\begin{aligned} p_k(\Delta v_f) &= \int_{-\infty}^{\infty} d\Delta v p_k(\Delta v_f | \Delta v) P(\Delta v) \\ &= \frac{1}{\beta} \frac{1}{\Delta v_f} \int_{\Delta v_f}^{\infty} d\Delta v P(\Delta v), \end{aligned} \quad (8)$$

where $P(\Delta v)$ is the probability distribution for the kick velocity, given by Eq. (2) with standard deviation $\sigma = \sqrt{2\beta}$.

The total velocity at the end of the time interval, $v_f = \Delta v_f + \tilde{v}$ is the sum of two terms, the kick velocity and the velocity from the start of the interval, v_i , propagated in time to the end of the interval, $\tilde{v} = v_i e^{-\beta}$. Given the distribution of the initial velocities $f_i(v_i)$, the distribution of final velocities (without kick) is given by $\tilde{f}(\tilde{v}) = f_i(\tilde{v} e^{\beta}) e^{\beta}$. Since the two velocity contributions Δv_f and \tilde{v} are statistically independent, the probability distribution of the sum is given by the convolution: $f(v_f) = (p_k * \tilde{f})(v_f)$. In the stationary state, we require that the initial velocity distribution is equal to the final velocity distribution,

$$f(v) = \int_{-\infty}^{\infty} du p_k(v - u) f(u e^{\beta}) e^{\beta}. \quad (9)$$

The probability distribution within this single-particle model is a function of $\beta = \gamma/f_{Dr}$ only, which matches the behavior of the many-particle simulation data. With the Fourier transform $\hat{f}(k) \equiv \int dv e^{ikv} f(v)$, the above equation simplifies,

$$\hat{f}(k) = \hat{p}_k(k) \hat{f}(k e^{-\beta}), \quad (10)$$

and is solved by

$$\hat{f}(k) = \prod_{j=0}^{\infty} \hat{p}_k(k e^{-j\beta}) \quad (11)$$

with

$$\hat{p}_k(k) = \int_0^1 dw \exp\left(-\frac{1}{2}k^2\sigma^2 e^{-2\beta w}\right). \quad (12)$$

For a given β , the infinite product can be truncated for some value of $j \gg 1/\beta$.

We now analyze the behavior of this formal solution, Eq. (11), in the limits of large and small β , where we can obtain simple analytic expressions for $f(v)$, and for intermediate values of β , where we obtain the distribution through an iterative numerical method.

First, in the $\beta \rightarrow 0$ limit, the Δv_f distribution $p_k(\Delta v_f)$ goes to $P(\Delta v_f)$, which is a Gaussian. Thus, according to Eq. (9), the velocity distribution $f(v)$ must map to itself under a convolution with a Gaussian, which requires that $f(v)$ must itself be a Gaussian. This stationary limit corresponds to a continuous Ornstein-Uhlenbeck process [27]. The cumulant relation [28] implied by Eq. (11) specifies that the variance of $f(v)$ goes to unity as $\beta \rightarrow 0$. This is confirmed by the simulations with $\beta = 0.1$, shown in Fig. 1.

Second, in the large β limit, only the $j = 0$ term in Eq. (11) contributes to the product, and so $f(v) = p_k(v)$. As such, from Eq. (8), we can identify three regions

$$f(v) \approx \begin{cases} \frac{e^\beta - 1}{2\sqrt{\pi\beta^3}} & |v| \ll \sigma e^{-\beta} \\ \frac{1}{2\beta|v|} & \sigma e^{-\beta} \ll |v| \ll \sigma \\ \frac{1}{\sqrt{\pi\beta}} \frac{1}{v^2} e^{-v^2/4\beta} & |v| \gg \sigma \end{cases} \quad (13)$$

The middle case corresponds to taking the integration range in Eq. (8) to be zero to infinity (for positive Δv_f). The top case corresponds to a smooth cutoff to the $1/|\Delta v_f|$ behavior as $\Delta v_f \rightarrow 0$. The large Δv_f limit is obtained by setting the upper integration limit to infinity, giving the complementary error function. In Fig. 4 we plot the velocity distribution data for $\beta = 10$ and $\beta = 5$ and compare to the analytic expressions (dashed lines) from Eq. (13) and their ranges (dotted lines).

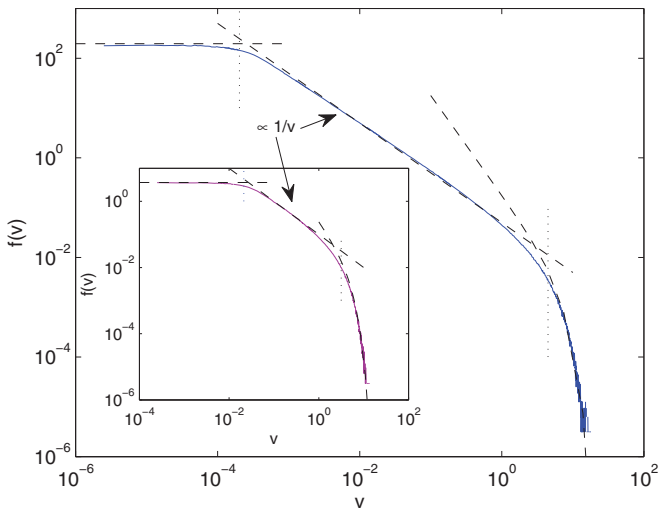


FIG. 4. (Color online) The three asymptotic solutions from Eq. (13) (dashed lines) and simulation data for $\beta = 10$, and $\beta = 5$ in the inset (both simulation data for $\eta = 0.35$). The dotted lines depict the range limits from Eq. (13). The dashed lines are the analytic results from Eq. (13), without any fitting.

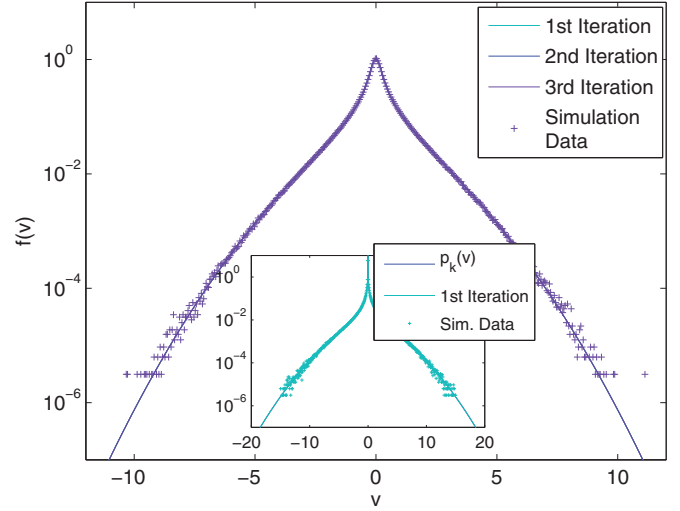


FIG. 5. (Color online) Main part: The first three iterations for $\beta = 3$ are almost indistinguishable and agree with the simulation data. Inset: First iteration and simulation data for $\beta = 10$, and $p_k(v)$, which is indistinguishable from the first iteration.

The three regions are clearly distinguishable and match the simulation data well. Note that the $1/|v|$ region shrinks as β decreases.

Third, for intermediate values of β we solved the defining Eq. (9) numerically by iteration, starting from a Maxwell-Boltzmann distribution. The convergence of the iteration process is very fast; there is almost no difference visible between the first three iterations (see Fig. 5). To quantify the difference between two subsequent iterations, we compute the \mathcal{L}^1 norm of $\Delta f(x) = f^{n+1}(x) - f^n(x)$. As an example, for $\beta = 3$ we find values of $\mathcal{O}(10^{-3})$ between the first and second iteration, and $\mathcal{O}(10^{-9})$ between the second and third iteration, respectively. The iterative solution of Eq. (9) is compared to the data from simulations for several values of β in Fig. 1. No deviations can be detected within the scatter of the data. We find similar good agreement for all values of β .

V. CONCLUSION

We have shown that a Brownian suspension of interacting particles, subjected to random accelerations, exhibits strongly anomalous velocity distributions. An event-driven algorithm was generalized to finite friction, allowing for large-scale simulations of over 2×10^6 particles. The simulations reveal velocity distributions, which are universal in the sense that they are largely independent of volume fraction and collisions between the particles, and only depend on damping rate and kick frequency through the ratio $\beta = \gamma/f_{Dr}$. This has led us to consider a simplified one-particle model allowing for an analytical theory of the velocity distribution, $f(v)$. The resulting integral equation reduces trivially to the Maxwell-Boltzmann distribution for $\beta \rightarrow 0$. For large β , we find a divergent distribution for small argument, $f(0) \sim e^\beta$, a $1/v$ decay for intermediate v and Gaussian behavior for the largest argument. Hence there are no exponential tails. In Refs. [11,29] an exponential tail was obtained for a damped particle kicked by white shot noise, but in these works the kick

size distribution was exponential, rather than the Gaussian we use. For intermediate β , the integral equation for $f(x)$ is solved by iteration with very fast convergence. For all β we find excellent agreement between the one-particle theory and the simulations.

Power law velocity distributions are nontrivial solutions of the unforced Boltzmann equation [30], where dissipation is due to inelastic collisions and no damping with a medium is considered. In contrast, for elastic collisions as considered here, the solution of the Boltzmann equation is of course the Maxwell-Boltzmann distribution. Hence the origin of the algebraic decay of the velocity distribution observed in the present work is distinct from that of Ref. [30].

Our approach can be generalized in several ways. Both the simulations as well as the analytical theory can be generalized to other distributions for the kick amplitudes and times. It also of interest to include dissipation in the collisions in order to make closer contact with experiments on granular media. Furthermore we plan to study directed motion, polar particles, and rotational degrees of freedom, modeling other swimmers.

ACKNOWLEDGMENTS

We thank C. Heussinger, W. T. Kranz, M. Müller, and M. Wardetzky for useful discussions. A.F. and A.Z. acknowledge support from DFG by FOR 1394.

-
- [1] E. Lauga and R. P. Powers, *Rep. Prog. Phys.* **72**, 096601 (2009).
 - [2] M. J. Lighthill, *Comm. Pure Appl. Math.* **5**, 109 (1952).
 - [3] C. Brennen and H. Winet, *Ann. Rev. Fluid Mech.* **9**, 339 (1977).
 - [4] R. Golestanian and A. Ajdari, *Phys. Rev. Lett.* **100**, 038101 (2008).
 - [5] A. Baskaran and M. C. Marchetti, *Proc. Natl. Acad. Sci. USA* **106**, 15567 (2009).
 - [6] H. H. Wensink and H. Löwen, *J. Phys. C* **24**, 460130 (2012).
 - [7] H.-R. Jiang, N. Yoshinaga, and M. Sano, *Phys. Rev. Lett.* **105**, 268302 (2010).
 - [8] A. Kudrolli, G. Lumay, D. Volfson, and L. S. Tsimring, *Phys. Rev. Lett.* **100**, 058001 (2008).
 - [9] A. Czirók, K. Schlett, E. Madarász, and T. Vicsek, *Phys. Rev. Lett.* **81**, 3038 (1998).
 - [10] A. Sokolov, M. Apodaca, B. Grzybowski, and I. Aranson, *Proc. Natl. Acad. Sci. USA* **107**, 969 (2010).
 - [11] P. Romaczuk, M. Bär, W. Ebeling, B. Lindner, and L. Schimansky-Geier, *Eur. Phys. J.* **202**, 1 (2012).
 - [12] I. Llopis and I. Pagonabarraga, *Europhys. Lett.* **75**, 999 (2007).
 - [13] M. Abbas, E. Clement, O. Simonin, and M. R. Maxey, *Phys. Fluids* **18**, 121504 (2006).
 - [14] P. Melby, F. V. Reyes, A. Prevost, R. Robertson, P. Kumar, D. A. Egolf, and J. S. Urbach, *J. Phys. C* **17**, S2689 (2005).
 - [15] A. Kudrolli and J. Henry, *Phys. Rev. E* **62**, R1489 (2000).
 - [16] J. S. van Zon, J. Kreft, D. I. Goldman, D. Miracle, J. B. Swift, and H. L. Swinney, *Phys. Rev. E* **70**, 040301 (2004).
 - [17] P. M. Reis, R. A. Ingale, and M. D. Shattuck, *Phys. Rev. E* **75**, 051311 (2007).
 - [18] H.-Q. Wang, K. Feitosa, and N. Menon, *Phys. Rev. E* **80**, 060304(R) (2009).
 - [19] K. Kohlstedt, A. Snezhko, M. V. Sapozhnikov, I. S. Aranson, J. S. Olafsen, and E. Ben-Naim, *Phys. Rev. Lett.* **95**, 068001 (2005).
 - [20] J. Harting, H. Herrmann, and E. Ben-Naim, *Europhys. Lett.* **83**, 30001 (2008).
 - [21] H. C. Berg, *E. Coli in Motion*, Vol. 18 (Springer, New York, 2004).
 - [22] J. Tailleur and M. E. Cates, *Phys. Rev. Lett.* **100**, 218103 (2008).
 - [23] R. R. Bennett and R. Golestanian, *Phys. Rev. Lett.* **110**, 148102 (2013).
 - [24] B. Alder and T. Wainwright, *J. Chem. Phys.* **31**, 459 (1959).
 - [25] B. Lubachevsky, *J. Comput. Phys.* **94**, 255 (1991).
 - [26] A. Fiege, M. Grob, and A. Zippelius, *Granular Matter* **14**, 247 (2012).
 - [27] N. G. Van Kampen, *Stochastic Processes in Physics and Chemistry*, Vol. 1 (North Holland, Netherlands, 1992).
 - [28] The product solution Eq. (11) implies the relation $\kappa_n^f = \kappa_n^p / (1 - e^{-n\beta})$ between the n th cumulants of f and p_k .
 - [29] C. Van Den Broeck, *J. Stat. Phys.* **31**, 467 (1983).
 - [30] E. Ben-Naim, B. Machta, and J. Machta, *Phys. Rev. E* **72**, 021302 (2005).